JOURNAL OF GEOPHYSICAL RESEARCH, VOL. 88, NO. C11, PAGES 6611–6621, AUGUST 20, 1983

A Dynamic Model for the Production of H^+, NO_3^-, and SO_4^{2-} in Urban Fog

DANIEL J. JACOB AND MICHAEL R. HOFFMANN

Environmental Engineering Science, W. M. Keck Laboratories, California Institute of Technology, Pasadena, California 91125

The chemical composition of nighttime urban fog has been investigated using a hybrid kinetic and equilibrium model. Extremely high acidity may be imparted to the droplets by condensation and growth on acidic condensation nuclei or by in situ S(IV) oxidation. Important oxidants of S(IV) were found to be O_2 as catalyzed by Fe(III) and Mn(II), H_2O_2, and O_3. Formation of hydroxymethanesulfonate ion (HMSA) via the nucleophilic addition of HSO_3^- to CH_2O(l) significantly increased the droplet capacity for S(IV) but did not slow down the net S(IV) oxidation rate leading to fog acidification. Gas phase nitric acid, ammonia, and hydrogen peroxide were scavenged efficiently, although aqueous phase hydrogen peroxide was depleted rapidly by reduction with S(IV). Nitrate production in the aqueous phase was found to be dominated by HNO_3 gas phase scavenging. Major aqueous phase species concentrations were controlled primarily by condensation, evaporation, and *p*H.

INTRODUCTION

Concentrations of major ions in nonprecipitating clouds [*Hegg and Hobbs*, 1981] and fogs [*Waldman et al.*, 1982; *Munger et al.*, 1983] have been reported to be significantly higher than those commonly observed in acidic precipitation. In Los Angeles, fogwater [*Waldman et al.*, 1982; *Munger et al.*, 1983] was reported to have acidities 100 times higher than those observed previously in rainwater by *Liljestrand and Morgan* [1981]. Lower dilutions and higher scavenging efficiencies due to reduced mass transfer limitations of gas absorption and longer residence times may explain, in part, the higher concentrations found in fog (1–100 μm) than in rain (0.1–3.0 mm).

A number of rainwater and cloudwater chemistry models have been proposed recently. *Adamowicz* [1979] simulated the chemistry of raindrops falling through a well-mixed polluted layer with uniform and constant concentrations of SO_2, CO_2, and NH_3. Gas and aqueous phase equilibria were established at all times, and aqueous phase transformation of S(IV) to S(VI) was allowed to proceed through the iron-catalyzed oxidation by O_2 according to the kinetic expression of *Brimblecombe and Spedding* [1974]. Mass transfer at the surface of the drop was modeled by two-film theory, but *Baboolal et al.* [1981] have since shown this simple model to be unsatisfactory since it ignores forced convection inside and outside of the falling drop. *Durham et al.* [1981] added NO_x to the gas phase and allowed some NO_x gas phase chemistry, considered kinetic expressions for all reactions instead of equilibrium relationships, and assumed O_3 to be the only liquid phase oxidant of S(IV) using the rate law of *Erickson et al.* [1977]. *Easter and Hobbs* [1974] modeled cloudwater chemistry by using a wave cloud model, an open atmosphere with trace concentrations of CO_2, SO_2, and NH_3, and a rudimentary S(IV) oxidation rate consisting of a simple first-order dependence on sulfite. More recent models have been proposed by *Middleton et al.* [1980], *Chameides and Davis* [1982], and *Carmichael et al.* [1983].

With this work in mind, a dynamic model for fogwater chemistry has been developed. The model has a hybrid kinetic and equilibrium structure: reactions which rapidly come to equilibrium are considered separately from reactions that are kinetically controlled. Gas phase chemistry, particle scavenging by droplets, evolution of the droplet microphysics, and deposition were not included explicitly.

Copyright 1983 by the American Geophysical Union.

Paper number 3C0722.
0148-0227/83/003C-0722$05.00

STRUCTURE OF THE MODEL

Aqueous Phase Reactions

The chemical composition of a fog droplet is assumed to be determined by the following factors: (1) the composition of the activated cloud condensation nuclei (CCN) on which the droplet condenses, (2) the absorption of atmospheric gases at the droplet surface, and (3) the subsequent aqueous phase reactions of homogeneous and heterogeneous species. Proton transfer and most ligand substitution reactions proceed extremely fast compared to the time scales of interest in this study [*Hoffmann*, 1981]; therefore they are treated as dynamic equilibria. The same assumption is applied to gas absorption in accordance with Henry's law, although mass transfer may be retarded by the formation of an organic film at the droplet surface [*Graedel et al.*, 1983]. Equilibrium constants K_T have been adjusted for temperature T with the van't Hoff relationship:

$$\int_{K_{298}}^{K_T} d \ln K = \frac{\Delta H^\circ_{298}}{R} \int_{298}^{T} \frac{dT}{T^2} \qquad (1)$$

ΔH° values at 298°K were obtained from literature sources (see Table 1). The equilibrium composition was determined using a MINEQL subroutine [*Morel and Morgan*, 1972; *Westall et al.*, 1976]. In MINEQL the equilibrium constant approach is used to solve the chemical equilibrium problem, which is defined by a system of mass action equations. The computed concentrations of constituents are constrained to remain positive and to satisfy mole balance relationships provided by the analytical information. Given a set of chemical constituents which have been defined operationally as metals and ligands, along with the corresponding stoichiometric and thermodynamic data, all the possible chemical species in a model system can be defined. The concentrations of these chemical species are written as functions of the free con-

TABLE 1. Henry's Law and Aqueous-Phase Equilibria Relevant to the Droplet Chemistry

Reaction No.	Reaction	pK*	$\Delta H^\circ_{298.15}$, kcal mole^{-1}	Reference†
(R1)	$H_2O(l) \rightleftharpoons H^+ + OH^-$	14.00	13.35	SM
(R2)	$SO_2(g) + H_2O \rightleftharpoons SO_2 \cdot H_2O$	−0.095	−6.25	SM
(R3)	$SO_2 \cdot H_2O \rightleftharpoons H^+ + HSO_3^-$	1.89	−4.16	SM
(R4)	$HSO_3^- \rightleftharpoons H^+ + SO_3^{2-}$	7.22	−2.23	SM
(R5)	$HNO_3(g) \rightleftharpoons H^+ + NO_3^-$	−6.51	−17.3	SW
(R6)	$HNO_2(g) \rightleftharpoons HNO_2(l)$	−1.7	−9.5	SW
(R7)	$HNO_2(l) \rightleftharpoons H^+ + NO_2^-$	3.29	2.5	SW
(R8)	$CO_2(g) + H_2O \rightleftharpoons CO_2 \cdot H_2O$	1.47	−4.85	SM
(R9)	$CO_2 \cdot H_2O \rightleftharpoons H^+ + HCO_3^-$	6.37	1.83	SM
(R10)	$HCO_3^- \rightleftharpoons H^+ + CO_3^{2-}$	10.33	3.55	SM
(R11)	$CH_2O(g) + H_2O \rightleftharpoons CH_2O \cdot H_2O$	−3.85	−12.85	LB
(R12)	$HOCH_2SO_3H \rightleftharpoons H^+ + HOCH_2SO_3^-$	<0‡	U§	R
(R13)	$HOCH_2SO_3^- \rightleftharpoons H^+ + {}^-OCH_2SO_3^-$	11.7	U	SA
(R14)	$NH_3(g) + H_2O \rightleftharpoons NH_3 \cdot H_2O$	−1.77	−8.17	SM
(R15)	$NH_3 \cdot H_2O \rightleftharpoons NH_4^+ + OH^-$	4.77	0.9	SM
(R16)	$O_2(g) \rightleftharpoons O_2(l)$	2.90	−3.58	P
(R17)	$H_2O_2(g) \rightleftharpoons H_2O_2(l)$	−4.85	−14.5	MD
(R18)	$O_3(g) \rightleftharpoons O_3(l)$	2.03	−5.04	L-B
(R19)	$CaHCO_3^+ \rightleftharpoons Ca^{2+} + HCO_3^-$	11.6	−2.78	SM
(R20)	$CaSO_4(l) \rightleftharpoons Ca^{2+} + SO_4^{2-}$	2.30	−1.65	SM
(R21)	$NaSO_4^- \rightleftharpoons Na^+ + SO_4^{2-}$	0.70	−2.23	SM
(R22)	$FeSO_4^+ \rightleftharpoons Fe^{3+} + SO_4^{2-}$	4.20	5.4	SM
(R23)	$Fe(SO_4)_2^- \rightleftharpoons Fe^{3+} + 2SO_4^{2-}$	5.60	U	SM
(R24)	$FeCl^{2+} \rightleftharpoons Fe^{3+} + Cl^-$	1.40	−7.91	SM
(R25)	$FeOH^{2+} \rightleftharpoons Fe^{3+} + OH^-$	12.30	0.04	SM
(R26)	$Fe(OH)_2^+ \rightleftharpoons Fe^{3+} + 2OH^-$	23.3	U	SM
(R27)	$Fe(OH)_3\downarrow \rightleftharpoons Fe^{3+} + 3OH^-$	39.0	20.7	SM
(R28)	$Fe_2(OH)_2^{4+} \rightleftharpoons 2Fe^{3+} + 2OH^-$	25.7	16.2	SM
(R29)	$FeSO_3^+ \rightleftharpoons Fe^{3+} + SO_3^{2-}$	10.0	U	this laboratory
(R30)	$MnSO_4(l) \rightleftharpoons Mn^{2+} + SO_4^{2-}$	2.30	−3.39	SM
(R31)	$MnCl^+ \rightleftharpoons Mn^{2+} + Cl^-$	1.10	−8.01	SM
(R32)	$HSO_4^- \rightleftharpoons H^+ + SO_4^{2-}$	2.20	−4.91	SM

*K is in M atm^{-1} or M". Temperature is 298°K.

†Reference code: SM = *Sillén and Martell* [1964]; SW = *Schwartz and White* [1981]; LB = *Ledbury and Blair* [1925]; SA = *Sørensen and Andersen* [1970]; MD = *Martin and Damschen* [1981]; L-B = *Landolt-Börnstein* [1976]; R = *Roberts et al.* [1971]; P = *Perry* [1963].

‡The pK for this reaction is very low.

§Unknown, $\Delta H = 0$ is assumed in the calculation.

centrations of the constituents by mass action equations. These functions are substituted into the mole balance equations with elimination of solids. The problem is reduced to a system of nonlinear equations in which the unknowns are the concentrations of the metals and ligands. This system of equations is solved by the Newton-Raphson method. The initial solution is tested against the solubility products of the solids and a new set of solids, which includes those solids with the most exceeded solubility products, is selected for the next computation. A final solution is achieved when the difference between the imposed analytical concentrations for a constituent and the sum of all individual species containing that constituent is less than or equal to a set value which is very small. Corrections for ionic strength were made using the Davies equation [*Stumm and Morgan*, 1981]. The thermodynamic data base consisted of 1300 equilibria; those found to influence the droplet composition are listed in Table 1.

For slower reactions, empirical rate laws were used. Specific rate laws for oxidation reactions involving N(III) and S(IV) have been incorporated in the model; they are listed in Table 2. Hydrogen peroxide, N(III), and O_3 are potentially important oxidants, and O_2 may also be important if catalyzed by active sites on soot or by transition metals, such as Fe(III) and Mn(II). Iron(III) and manganese(II) are effective catalysts when dissolved as free ions or complexes [*Hoffmann and Jacob*, 1983] but their catalytic properties are altered if they are present as solid phases. Surface catalysis may occur but in the absence of reliable data it has been neglected. In the kinetic formulation of (R35), [Fe(III)] and [Mn(II)] represent the summation of concentrations of all dissolved iron and manganese species. It should be noted that the kinetic data for this reaction is not satisfactory around pH 4 because of the influence of $Fe(OH)_3(s)$ which starts dissolving near pH 4. Rate expressions given by *Martin* [1983] at high pH and low pH fail to extrapolate to the same value at intermediate pH. To minimize this problem, an average of the two expressions was used near pH 4.

The reactions of absorption and aqueous phase disproportionation of NO_x to form nitrous and nitric acid have been reviewed by *Schwartz and White* [1981]. These reactions could be major contributors to nitrate formation in fog droplets if allowed to reach equilibrium; however, because of second-order kinetics they are too slow to be important on the time scales of concern in fog. Alternative aqueous phase nitrate formation pathways involve the oxidation of N(III) by H_2O_2 and O_3 [*Damschen and Martin*, 1982].

Overall, the rate laws shown in Table 2 indicate that oxidation reactions proceed on time scales of minutes to hours under urban atmospheric conditions. These rate laws are integrated with a simple finite difference scheme using adjustable

TABLE 2a. Kinetic Expressions for the Aqueous Phase Oxidation Reactions of S(IV) to S(VI) and N(III) to N(V)

Reaction No.	Reaction	Conditions	Rate, $M\ s^{-1}$ at 25°C*	Activation Energy, kcal $mole^{-1}$	Reference†
(R33)	$S(IV) + H_2O_2$		$\frac{d[S(VI)]}{dt} = \frac{8 \times 10^4[H_2O_2(l)][SO_2(l)]}{0.1 + [H^+]}$	7.3	M
(R34)	$S(IV) + O_3$	$pH < 3$	$\frac{d[S(VI)]}{dt} = \frac{1.9 \times 10^4[SO_2(aq)][O_3(l)]}{[H^+]^{1/2}}$	6	M
		$pH > 3$	$\frac{d[S(VI)]}{dt} = 4.19 \times 10^5\left(1 + \frac{2.39 \times 10^{-4}}{[H^+]}\right)[O_3(l)][SO_2(aq)]$	6	Ma
(R35)	$S(IV) + O_2$ (with Fe (III) and Mn(II))	$[SO_2(aq)] > 10^{-5}$, $pH < 4$	$\frac{d[S(VI)]}{dt} = \frac{4.7[Mn(II)]^2}{[H^+]} + \left(\frac{0.82[Fe(III)][SO_2(aq)]}{[H^+]} \cdot \left(1 + \frac{1.7 \times 10^3[Mn(II)]^{1.5}}{6.3 \times 10^{-6} + [Fe(III)]}\right)\right)$	21.8	M
		$[SO_2(aq)] < 10^{-5}$, $pH < 4$	$\frac{d[S(VI)]}{dt} = 3\left(5000[Mn(II)][HSO_3^-] + \frac{0.82[Fe(III)][SO_2(aq)]}{[H^+]}\right)$	21.8	M
		$[SO_2(aq)] > 10^{-5}$, $pH > 4$	$\frac{d[S(VI)]}{dt} = \frac{4.7[Mn(II)]^2}{[H^+]} + 1 \times 10^7[Fe(III)][SO_2(aq)]^2$	27.3	M
		$[SO_2(aq)] < 10^{-5}$, $pH > 4$	$\frac{d[S(VI)]}{dt} = 5000\ [Mn(II)][HSO_3^-]$	27.3	M
(R36)	$S(IV) + O_2$ (with soot)‡		$\frac{d[S(VI)]}{dt} = 2.54 \times 10^7[O_2(l)]^{0.69} \cdot C_x \frac{[SO_2(aq)]^2}{1 + 3.06 \times 10^6[SO_2(aq)] + 1.5 \times 10^{12}[SO_2(aq)]^2}$	11.7	B
(R37)	$S(IV) + N(III)$	$pH < 3$	$\frac{d[S(VI)]}{dt} = 142[H^+][HNO_2(aq)][SO_2(aq)]$	12§	M
		$pH > 3$	$\frac{d[S(VI)]}{dt} = 2.2[HNO_2(l)][HSO_3^-]$	12§	O
(R38)	$N(III) + H_2O_2$		$\frac{d[S(VI)]}{dt} = 4.6 \times 10^3[H^+][H_2O_2(l)][HNO_2(l)]$	13.2	DM
(R39)	$N(III) + O_3$		$\frac{d[S(VI)]}{dt} = 5 \times 10^5[O_3(l)][NO_2^-]$	13.8	DM

*$[SO_2(aq)] = [SO_2(l)] + [HSO_3^-] + [SO_3^{2-}]$; $[HNO_2(aq)] = [HNO_2(l)] + [NO_2^-]$.
†Reference code: M = *Martin* [1982]; Ma = *Maahs* [1982]; B = *Brodzinsky et al.* [1980]; O = *Oblath et al.* [1981]; DM = *Damschen and Martin* [1982].
‡C_x is the concentration of active carbon in g l^{-1}.
§Assumed.

time steps ranging from 10 s to 200 s:

$$[R_i]_{t+\Delta t} = [R_i]_t + \left(\sum_{ox}\left(\frac{d[R_i]}{dt}\right)_{ox}\right)\Delta t \tag{2}$$

where $[R_i]$ represents the concentration of the reduced component R_i (i.e. N(III) or S(IV)).

Of special interest in urban fog is the reaction of HSO_3^- with CH_2O and with other aldehydes, RCHO, to form hydroxymethanesulfonate ion (HMSA) and the corresponding sulfonates, $HOCHRSO_3^-$ [*Munger et al.*, 1983]:

$$CH_2O + HSO_3^- \underset{k_r}{\overset{k_f}{\rightleftharpoons}} HOCH_2SO_3^- \tag{3}$$

Dasgupta et al. [1980] determined a conditional equilibrium constant for HMSA to be $K_{298} = k_f/k_r = 7.5 \times 10^4\ M^{-1}$, while S. D. Boyce and M. R. Hoffmann (unpublished manuscript, 1983) have determined that $k_f = 3\ M^{-1}\ s^{-1}$. Production of HMSA will contribute to the droplet acidity indirectly by producing a droplet that is supersaturated with respect to SO_2(g), and because of the slow reversibility of (3), HMSA formation may inhibit the production of S(VI). Reaction (3) is integrated at each time step by using the integrated form of the rate law:

$$\ln\left|\frac{[HSO_3^-]_{t+\Delta t} - p}{[HSO_3^-]_{t+\Delta t} - q}\right| = k_f(q - p)\,\Delta t + \ln\left|\frac{[HSO_3^-]_t - p}{[HSO_3^-]_t - q}\right| \tag{4}$$

TABLE 2b. Reaction Stoichiometries for Reactions in Table 2a

Reaction No.	Reaction Stoichiometries
(R33)	$HSO_3^- + H_2O_2(l) \rightarrow HSO_4^- + H_2O$
(R34)	$HSO_3^- + O_3(l) \rightarrow HSO_4^- + O_2$
(R35)	$HSO_3^- + 1/2O_2(l) \rightarrow HSO_4^-$
(R37)	$2HNO_2(l) + H_2O \cdot SO_2 \rightarrow 2NO + H^+ + HSO_4^- + H_2O$ $2HNO_2(l) + 2H_2O \cdot SO_2 \rightarrow 2SO_4^{2-} + N_2O + H_2O + 4H^+$
(R38)	$HNO_2(l) + H_2O_2(l) \rightarrow NO_3^- + H_2O + H^+$
(R39)	$NO_2^- + O_3(l) \rightarrow NO_3^- + O_2$

$$[HMSA]_{t+\Delta t} = [HMSA]_t - ([HSO_3^-]_{t+\Delta t} - [HSO_3^-]_t) \quad (5)$$

where p and q are the solutions to the second-degree equation

$$KX^2 + (K([CH_2O(l)]_t - [HSO_3^-]_t) + 1)X - ([HSO_3^-]_t + [HMSA]_t = 0 \quad (6)$$

Gas Phase and Aerosol

At night the oxidation of nitrogeneous compounds and alkenes by ozone is important. The kinetics of these reactions are dependent on the downward diffusion of ozone to the boundary layer [*McRae*, 1981]. In the boundary layer, nitric acid may be produced [*Graham and Johnston*, 1978; *McRae and Russell*, 1983] by a variety of pathways. No attempt has been made to model gas phase chemistry. Instead, concentrations of gases and gas phase production rates (from emissions and homogeneous reactions) have been estimated from local field data and predictions from the Caltech air quality model for the Los Angeles basin [*McRae*, 1981].

The integrated mass and composition of the activated cloud condensation nuclei on which the fog droplets condense were estimated from field data. No subsequent scavenging of the interstitial aerosol by diffusion or impaction was considered.

Physical Description

A parcel of air is followed in which droplets form and grow by accretion of water vapor. The droplets are assumed to remain constantly within the air parcel (i.e., sedimentation and diffusion of the droplets are ignored).

The limitation of S(IV) oxidation rates by mass transfer has been discussed by *Schwartz and Freiberg* [1981] and *Baboolal et al.* [1981]. Schwartz and Freiberg have shown that for stationary droplets smaller than 50 μm the net rate of oxidation was limited strictly by oxidation. Baboolal et al. extended this analysis to droplets larger than 50 μm. These large droplets have a significant sedimentation velocity, which drives convection both inside and outside of the droplet. This mixing effect enhances the rate of mass transfer as calculated for stationary droplets. Therefore the chemical changes in fog droplets are most likely limited by the specific reaction rates.

Because fogs are localized events and occur on time scales of a few hours, advection of condensing and evaporating droplets can be ignored as a first approximation. Also, evolution of the droplet spectrum through coagulation can be neglected since mass transfer does not limit overall reaction rates. In this context the liquid water content of the air parcel and its time dependency are sufficient parameters for characterizing fog microphysics.

At $t = 0$, droplets are assumed to condense, receive an initial chemical loading from the water-soluble fraction of the activated nuclei, and immediately react with the gaseous environment. The growth and evaporation of the droplets is simulated by the external input of an evolving liquid water content. At each time step the equilibrium composition of the droplet is calculated along with the HMSA formation rate and the changes in component concentrations due to oxidation reactions.

RESULTS AND DISCUSSION

Sulfate and Nitrate Oxidation Pathways

In this section the relative contributions of the various S(IV) and N(III) oxidation mechanisms to the droplet chemistry are discussed. For this specific purpose a closed parcel of air with a constant liquid water content has been assumed (i.e., droplets condense on the activated condensation nuclei at $t = 0$ with no droplet growth or evaporation). A nighttime air mass typical of the industralized coastline of the Los Angeles basin has been chosen. Concentrations of gases and preexisting nuclei were estimated from local field data and transport models (Table 3). Gases are depleted by absorption except for CO_2 and O_2, which are held constant at a fixed partial pressure. The liquid water content is $L = 0.1$ g m^{-3} and the temperature is $T = 283$ K.

Kinetic results shown in Figure 1 clearly show that H_2O_2 and O_2 (catalyzed by Fe and Mn) are the principal oxidants for S(VI) production in situ. Hydrogen peroxide is highly soluble in water and rapidly oxidizes S(IV) at low pH; however, if not replenished, it is quickly depleted from the parcel of air by reduction to water. In this case, in the absence of gas phase or aqueous phase H_2O_2 formation, no H_2O_2 remains in the system after 10 minutes.

The catalytic effectiveness of both Fe(III) and Mn(II) is dependent on their speciation in the droplet (Figure 2). The principal manganese species are $Mn(H_2O)_6^{2+}$ and $MnSO_4$(aq). Both of these species are assumed to be equally effective as catalysts for S(IV) autoxidation. On the other hand, Fe(III) above pH 4 is found primarily as an iron(III) hydroxide solid, which has been assumed to be catalytically inactive. As the pH decreases below 4, the solid phase dissolves and soluble Fe(III), the active catalyst, is released. The rate law indicates a decrease of the oxidation rate with pH but the dissolution of Fe(III) at low pH offsets this effect and the calculated rate actually increases between pH 4 and 3.5.

Oxidation by ozone contributes ~4% of the total S(VI)

TABLE 3. Composition of the Air Mass (Trace Gases and Condensation Nuclei) Prior to Fog Formation at a Polluted Site

Atmospheric Trace Gases		
	Concentration, ppb	Reference
SO_2	20	SCAQMD data*
HNO_2	1	*Hanst et al.* [1982]
HNO_3	3	id.
NH_3	5	id.
CH_2O	30	*Grosjean* [1982]
O_3	10	SCAQMD data
H_2O_2	1	*Graedel et al.* [1976]

Condensation Nuclei†			
	Concentration μg m^{-3}		Concentration, μg m^{-3}
SO_4^{2-}	10	NH_4^+	6.65
NO_3^-	10	Na^+	.61
Cl^-	1.1	Fe(III)	.5
CO_3^{2-}	1.83	Mn(II)	.02
C_x(soot)	30	Ca^{2+}	1.22

The air mass is typical of the industrial coastline of the Los Angeles basin for an inversion height of about 50 m. $P_{O_2} = 0.21$ atm, $P_{CO_2} = 330$ ppm.

*Data from the permanent records of the South Coast Air Quality Management District.

†$(NH_4)_2SO_4$, NH_4NO_3, NaCl, $CaCO_3$, metal oxides, and soot. References: *Gartrell et al.* [1980]; *Appel et al.* [1980].

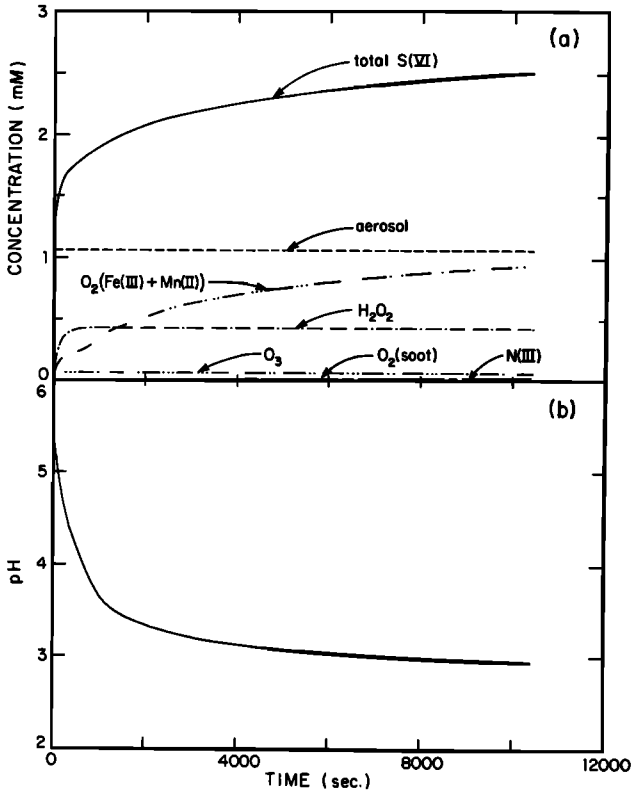

Fig. 1. (*a*) Profile versus time of total sulfate in the fogwater and of the individual contributions to the total sulfate of sulfate aerosol and different S(IV) oxidants. (*b*) Profile of *p*H versus time. The fog formed under the conditions of Table 3, with liquid water content = 0.1 g m^{-3}, temperature = 10°C.

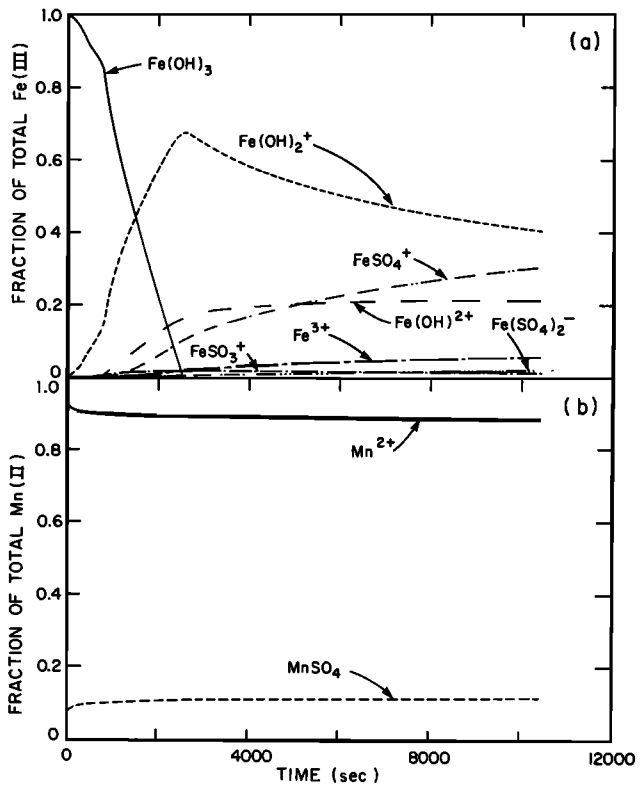

Fig. 2. Speciation of (*a*) Fe(III) and (*b*) Mn(II) in the fogwater as a function of time under conditions of Table 3, with liquid water content = 0.1 g m^{-3} and temperature = 10°C.

produced after 3 hours of fog. This is due to the low water solubility of ozone and the reciprocal hydrogen ion dependency of its reaction rate. Therefore little oxidation by ozone occurs below *p*H 4. Catalytic carbon sites in soot contribute <5% of the total S(VI) produced, even at the high carbon levels of urban environments. Oxidation by N(III) appears to be insignificant due to the low solubility of HNO_2(g) at *p*H < 4.

Oxidation of N(III) does not contribute appreciably to nitrate production. At t = 180 minutes, reaction with O_3 had generated less than 10^{-7} M NO_3^- and reaction with H_2O_2 less than 10^{-10} M NO_3^-.

The aqueous phase oxidation of S(IV) has an important consequence on the droplet acidity. Between *p*H 2 and 6 the principal reactive species of S(IV) is HSO_3^- [*Hoffmann and Jacob*, 1983]. The oxidation product, HSO_4^-, is completely dissociated above *p*H 3. Therefore the oxidation directly produces one free proton. Depletion of HSO_3^- leads to further dissolution of SO_2(g) which then dissociates to give HSO_3^- and H^+ in the droplet. Because the solubility of SO_2 decreases with *p*H, each depleted HSO_3^- molecule is not replaced in the droplet. Depending on the overall droplet chemistry, oxidation of one molar unit of S(IV) thus leads to the production of one- to two-fold that molar unit of free acidity. The impact on the droplet *p*H is dramatic, as shown in Figure 1*b*. In the first half hour of the fog, S(VI) production is the fastest and causes a *p*H drop of over two units. Field observations are consistent with these predictions [*Munger et al.*, 1983].

Components in the gas phase are scavenged by the droplets with efficiencies dependent on their Henry's law constants and aqueous phase chemistry. Table 4 shows the fraction of each gas scavenged at t = 0, t = 30 min, and t = 180 min. It must be kept in mind that these numbers vary with the liquid water content of the fog [*Schwartz*, 1983]. Nitric acid is totally dissolved and dissociated, while NH_3 dissolves totally at *p*H < 5. These two components essentially titrate each other in the aqueous phase. Formation of HMSA over the course of a fog event was found not to significantly increase the fraction of CH_2O scavenged; therefore the CH_2O partial pressure remains approximately constant throughout the simulation. Likewise, hydroxymethanesulfonate formation cannot be a significant sink for gas phase SO_2. The solubility of SO_2 is limited, but because $SO_2 \cdot H_2O$ is a weak acid, ~5% dissolves with the formation of the fog. S(IV) oxidation reactions further increase the fraction scavenged over the lifetime of the fog. Three hours after fog formation, over 80% of the initial SO_2 still remains in the gas phase, indicating that fog has little impact on the gaseous SO_2 concentration. Hydrogen peroxide

TABLE 4. Scavenging of Gases by Fog Droplets Under Conditions of Table 3

Gas	Fraction Scavenged From Gas Phase, %		
	t = 0	t = 30 min	t = 180 min
HNO_3	100	100	100
NH_3	43.9	99.5	100
CH_2O	5.0	5.3	5.3
SO_2	2.7	11.8	17.5
H_2O_2	32.1	100	100
O_3	0.0	1.5	1.5
HNO_2	3.8	0.0	0.0

Liquid water content = 0.1 g m^{-3}, temperature = 283 K.

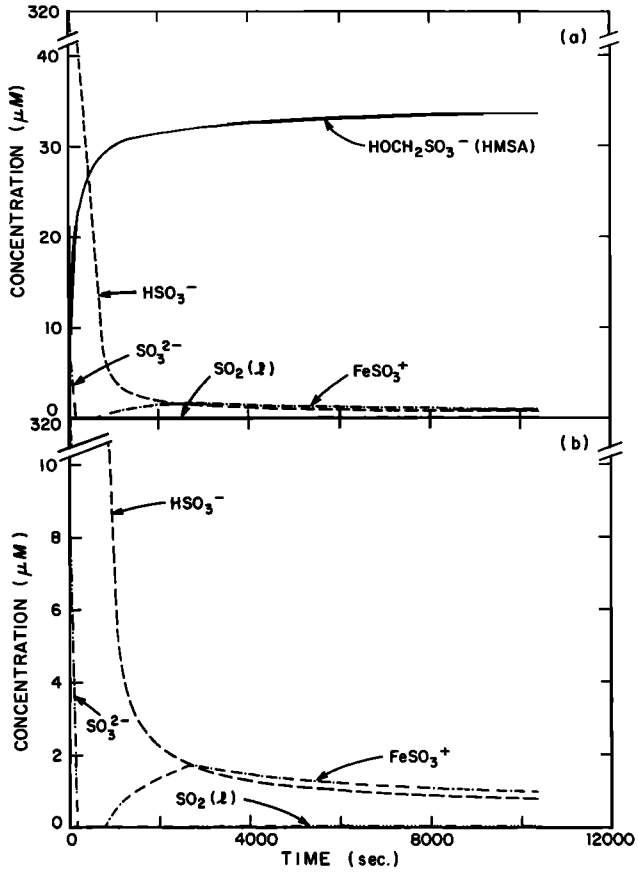

Fig. 3. (*a*) Concentrations of S(IV) species in the fogwater as a function of time under conditions of Table 3, with liquid water content = 0.1 g m^{-3} and temperature = 10°C. (*b*) Same as (*a*) but with no formaldehyde in the atmosphere.

is highly soluble in water. As was discussed above, reduction of H_2O_2 in the droplet is an efficient sink which depletes H_2O_2 from the system. Ozone, on the other hand, is poorly scavenged, as is HNO_2. Both react slowly in the droplet below *p*H 4.

The impact of HMSA formation on the droplet chemistry is worth discussing in some detail, as it has been the subject of recent interest [*Munger et al.*, 1983; *Boyce and Hoffmann*, 1983; *Richards et al.*, 1983]. Figure 3*a* shows the concentration profiles versus time for HSO_3^- and HMSA. The formation of HMSA is rapid but still slower than S(IV) oxidation. Consequently, the amount of HMSA produced is smaller than that of sulfate. Hydroxymethanesulfonate is the most important S(IV) species in solution; if formaldehyde was not present, the S(IV) concentration in the droplet would be much lower (Figure 3*b*).

It has been suggested that HMSA may inhibit S(IV) oxidation in atmospheric droplets by limiting the availability of reactive S(IV) species. This does not appear to be the case, since oxidation proceeds faster than adduct formation; furthermore, since the partial pressure of SO_2 remains approximately constant throughout the fog, the limiting concentrations of reactive S(IV) species are independent of the HMSA formation rate. However, the direct effect of HMSA on the fogwater acidity is of interest. Hydroxymethanesulfonate is the conjugate base of hydroxymethanesulfonic acid, which is a strong acid [*Roberts et al.*, 1971]. Hydroxymethanesulfonate is a weak acid (see Table 1). Between *p*H 2 and 10 and in a system open to SO_2, HMSA is stable and complexation of HSO_3^- leads to further dissolution of SO_2, which then dissociates and releases free acidity in the droplet. Because of the small amounts of HMSA produced with respect to the droplet $[H^+]$ concentration, this contribution is small.

In the first simulation, S(VI) formation buffered the droplet acidity at about *p*H 3, whereas in some extremely polluted atmospheres, higher acidity can be imparted to the droplet at $t = 0$ by simple dissolution of the activated nuclei. *Cass* [1975] reports some cases for Los Angeles, mostly under high humidity conditions, where the aerosol sulfate concentration was as high as 75 μg m^{-3}. A second simulation was run (Figures 4 and 5) under the same conditions as the first but with 75 μg m^{-3} SO_4^{2-} in the air mass as NH_4HSO_4 nuclei instead of 10 μg m^{-3} SO_4^{2-} as $(NH_4)_2SO_4$.

The *p*H of 2.4 at $t = 0$ (Figure 4) indicates the impact of the acid nuclei. At this low *p*H there is very little S(IV) in the droplet (Figure 5) and the only S(IV) oxidation reaction to proceed at a significant rate is that with H_2O_2. Therefore less sulfate and hydrogen ion are produced in situ. In the case of acidic condensation nuclei the *p*H of the fog may be controlled strictly by the nuclei composition instead of by S(VI) aqueous phase production. It should be mentioned that fogwater *p*H in the range of 2 to 2.5 has been observed in the Los Angeles basin following heavy 'smog' days. The lowest *p*H recorded was 1.69 in a dissipating fog along the coastline; in that case the dilution was probably less than the $L = 0.1$ g m^{-3} considered in the simulation.

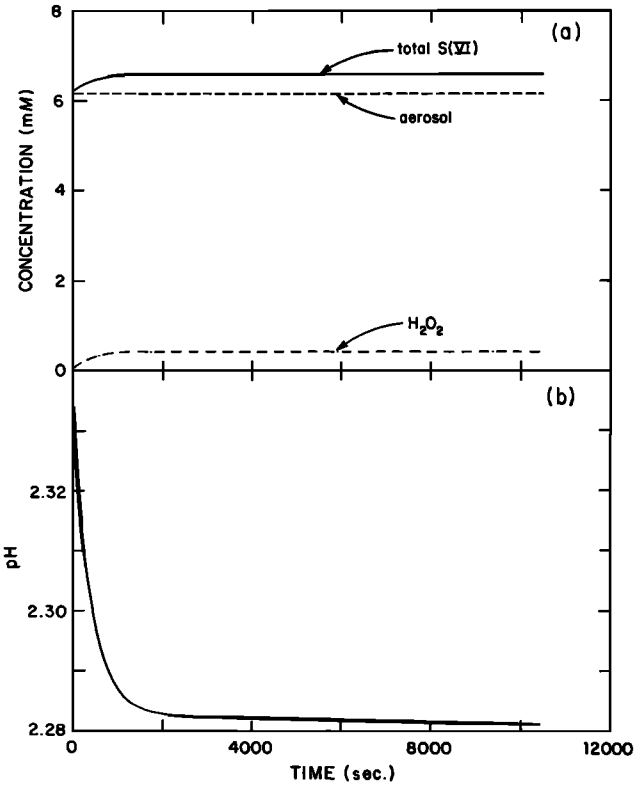

Fig. 4. (*a*) Profile versus time of total sulfate and of the individual contributions to the total sulfate of sulfate aerosol and different S(IV) oxidants. (*b*) Profile of *p*H versus time. The fog formed by condensation on highly acidic nuclei (75 μg m^{-3} NH_4HSO_4), other conditions as in Table 3, with liquid water content = 0.1 g m^{-3} and temperature = 10°C.

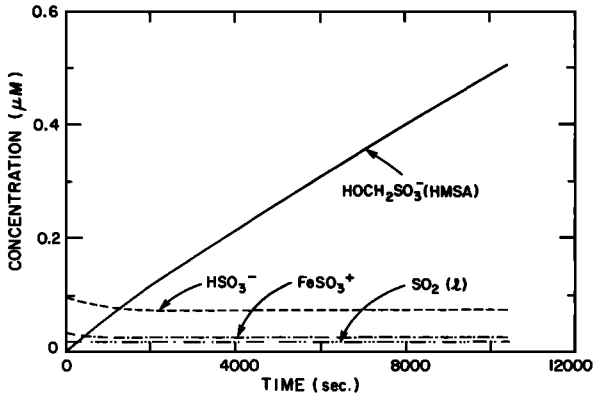

Fig. 5. Concentration of S(IV) species in the fogwater as a function of time. The fog formed by condensation on highly acidic nuclei (75 $\mu g\ m^{-3}$ NH_4HSO_4), other conditions as in Table 3, with liquid water content = 0.1 g m^{-3} and temperature = 10°C.

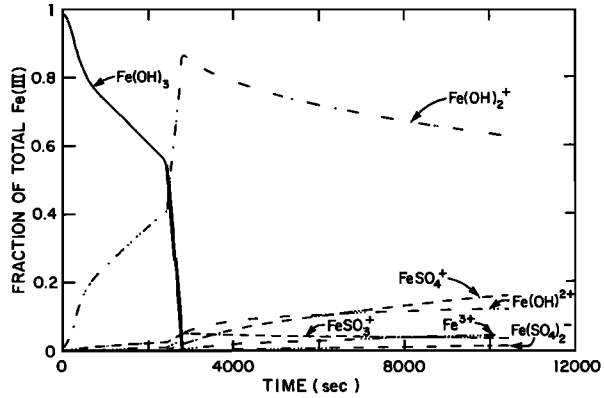

Fig. 7. Speciation of Fe(III) in the fogwater as a function of time under conditions of Table 3, with liquid water content = 0.1 g m^{-3} and temperature = 1°C.

Fog frequently forms at temperatures lower than 10°C. Radiation fogs, in particular, often form near freezing. To check the chemical sensitivity of the system to temperature, a simulation was run at 1°C with $L = 0.1$ g m^{-3} and conditions given in Table 3. Reaction rates are slower at 1°C, but gas solubility increases. Solution equilibria are shifted in either direction depending on the sign of $\Delta H°$. The combination of these effects has an interesting impact on the sulfate production rates and the *p*H profile (Figure 6). The rate of S(IV) oxidation by H_2O_2 is relatively unaffected because of its low activation energy E_a, but metal-catalyzed oxidation by O_2, which has a high E_a, is much slower at 1°C than at 10°C. Oxidation by ozone becomes appreciable at the beginning of the fog because of its low E_a and the increased ozone solubility. However, between *p*H 4.5 and *p*H 4, H_2O_2 is totally depleted and oxidation by ozone becomes insignificant; the S(IV) autoxidation reaction is also very slow. The sulfate concentration and *p*H profiles are almost at a plateau in this *p*H range. Then, as the *p*H drops below 4, $Fe(III)(OH)_3$ starts dissolving and the rate of oxidation by O_2 increases, such that sulfate and acidity are again produced at an appreciable rate. After 3 hours of fog the values for *p*H and sulfate concentration are close to what they were at 10°C. The speciation profile of Fe(III) (Figure 7) is similar to that at 10°C, but dissolution of $Fe(OH)_3$ is retarded because of the slow drop in *p*H from 4.5 to 4. The speciation of Mn(II) is essentially the same as at 10°C.

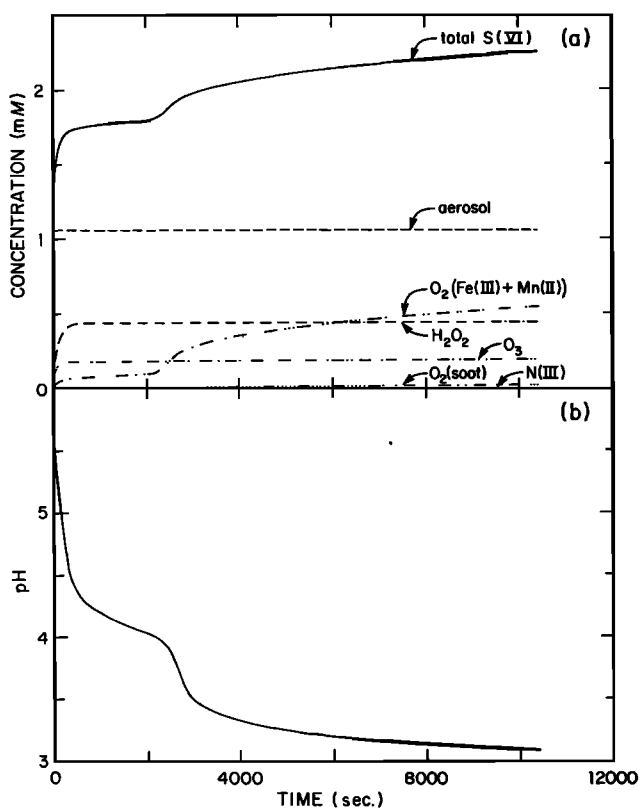

Fig. 6. (*a*) Profile versus time of total sulfate and of the individual contributions to the total sulfate of sulfate aerosol and different S(IV) oxidants. (*b*) Profile of *p*H versus time. The fog formed under the conditions of Table 3, with liquid water content = 0.1 g m^{-3} and temperature = 1°C.

The scavenging efficiency of gases (Table 5) reflects their increased solubility; however, because the aqueous phase reactions are slower, little increase is seen between $t = 0$ and $t = 30$ min. After 3 hours the scavenging efficiency for SO_2 is similar to that at 10°C.

An interesting feature of the chemistry at 1°C is the high concentration of HMSA (Figure 8), which is due to the increased solubility of SO_2 and CH_2O. The reaction proceeds via a nucleophilic substitution of methylene glycol (S. D. Boyce and M. R. Hoffmann, unpublished manuscript, 1983) with an activation energy near 12 kcal $mole^{-1}$. Consequently, the reaction still proceeds rapidly at 1°C.

TABLE 5. Scavenging of Gases by Fog Droplets Under Conditions of Table 3

Gas	Fraction Scavenged From Gas Phase, %		
	$t = 0$	$t = 30$ min	$t = 180$ min
HNO_3	100	100	100
NH_3	76.0	97.0	100
CH_2O	9.8	10.3	10.5
SO_2	10.7	13.0	18.2
H_2O_2	58.0	100	100
O_3	0.0	4.2	4.2
HNO_2	10.2	3.4	0.0

Liquid water content = 0.1 g m^{-3}; temperature = 274 K.

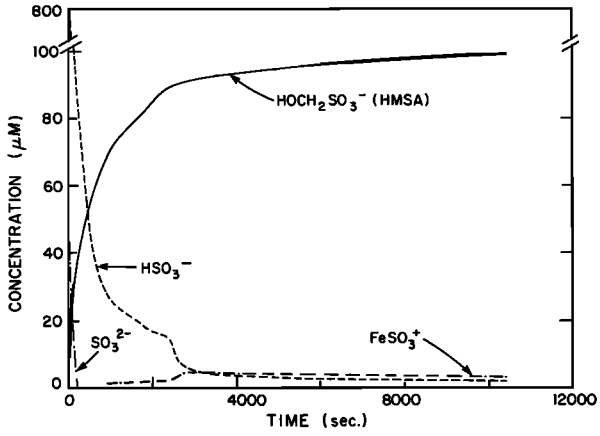

Fig. 8. Concentrations of S(IV) species in the fogwater as a function of time under conditions of Table 3, with liquid water content = 0.1 g m^{-3} and temperature = 1°C.

Simulation of a Fog Event

The simulation with the present model of an actual fog event necessitates the knowledge of input variables such as the condensation nuclei composition, the evolution of liquid water content with time, and the gas phase concentrations. Unfortunately, our field investigations [*Waldman et al.*, 1982; *Munger et al.*, 1983] so far have been limited to the determination of fogwater composition. Field data for the above parameters is incomplete; therefore a direct comparison of calculated and observed values is not possible at this time. In addition the current model neglects gas phase chemistry, transport mechanisms, and aerosol scavenging by droplets.

Fogwater composition and its variation with time for fog events at Lennox, a site in an industrial area near the Los Angeles coastline, have been documented thoroughly [*Waldman et al.*, 1982; *Munger et al.*, 1983]. In this section, a fog occurring under conditions typical of this highly impacted site has been simulated.

A plausible scenario for the evolution of liquid water content in fogs can be obtained from existing data [*Jiusto and Lala*, 1983]. The liquid water content often rises linearly following fog formation (neglecting small time scale oscillations), reaches a stable value after about an hour, and decreases linearly when the fog evaporates. Liquid water contents range from 0.01 g m^{-3} in very light fogs to 0.5 g m^{-3} in dense fogs. The profile chosen here is shown in Figure 9.

Concentrations of condensation nuclei and atmospheric gases prior to fog formation are given in Table 3. From the discussion of the previous section, it appears that some gas-phase emissions should be included. Hydrogen peroxide is not produced in the gas phase at night and thus actually disappears when the fog forms. Ammonia and HNO_3, which are scavenged efficiently by the droplets, are, on the other hand, continuously emitted into the atmosphere from a variety of sources. Because fog droplets are a sink for these two gases, fresh inputs into the parcel of air must be considered. At Lennox, plausible values associated with an inversion height of 50 m are 0.01 ppb min^{-1} for HNO_3 [*McRae and Russell*, 1983] and 0.01 ppb min^{-1} for NH_3 [*Russell et al.*, 1983]. Other gases included in the simulation are not depleted by fog, and a reasonable assumption is that their concentrations remain constant throughout the event. A constant temperature of 10°C has been chosen. Temperature changes during the course of fog events [*Jiusto and Lala*, 1983] are minimal.

The concentrations predicted for the major ions (Figure 10) are in the range of those reported by *Waldman et al.* [1982] and *Munger et al.* [1983], but no precise comparison should be made because of the reasons stated at the beginning of this section. The concave profiles observed (except for $[H^+]$) confirm the important role of dilution and evaporation that was suggested initially by Waldman et al. Aqueous phase oxidation of N(III) to N(V) is negligible and the only nitrate source is the slow gas phase production of HNO_3 followed by dissolution and dissociation. As a result, the nitrate concentration is controlled primarily by droplet growth. Similar behavior is predicted for ammonium ion, although in the initial stage of the fog the *p*H drop from a high value increases the NH_4^+ concentration. From equilibria described by (14) and (15), it is seen that scavenging of gaseous ammonia is highly *p*H-dependent over the range of 5 to 8, which is typical of fog forming in rural environments (D. J. Jacob, unpublished data, 1983) or influenced by alkaline atmospheric components [*Munger et al.*, 1983]. In such fogs, the NH_4^+ levels are expected to be controlled by acidity as well as dilution.

Oxidation of S(IV) contributes substantially to the sulfate level and the acidity in the early stages of the fog, and in the fully developed fog, 50% of the total sulfate present has been produced in the aqueous phase. During the first few minutes of the fog, S(IV) oxidation is in fact rapid enough to compensate for dilution; after H_2O_2 is depleted and the *p*H has dropped, the oxidation rate slows down and the role of dilution becomes predominant. Even with dilution the *p*H of the droplets does not rise because metal-catalyzed S(IV) oxidation by O_2 produces significant acidity in the droplet; instead, *p*H stabilizes at about 3.5. As the fog evaporates, concentration leads to a further *p*H decrease. The speciation of Fe(III) (Figure 11) correlates with *p*H in the manner discussed in the previous section. $FeSO_4^+$ becomes an important species as the fog evaporates because the sulfate concentration is so high. Speciation of Mn(II) (not shown) is similar to that in Figure 2.

An important question is, 'Is the sulfate formation predicted theoretically actually seen in the field?' The data of *Waldman et al.* [1982] and *Munger et al.* [1983] do not show obvious evidence for this. However, the bulk of the aqueous phase sulfate production is predicted to occur in the first hour of the fog, so that it could not be detected given the time resolution of the field study. A way to obtain experimental confirmation of this process would be to compare the amount of sulfate present in the atmosphere just before fog formation to that right after fog formation.

The HMSA concentration profile (Figure 12) shows the dominant effect of droplet growth and evaporation, except in

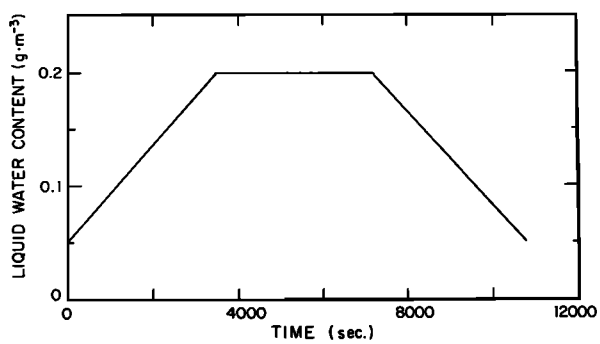

Fig. 9. Liquid water content profile versus time chosen for the simulation of a fog event in the Los Angeles basin.

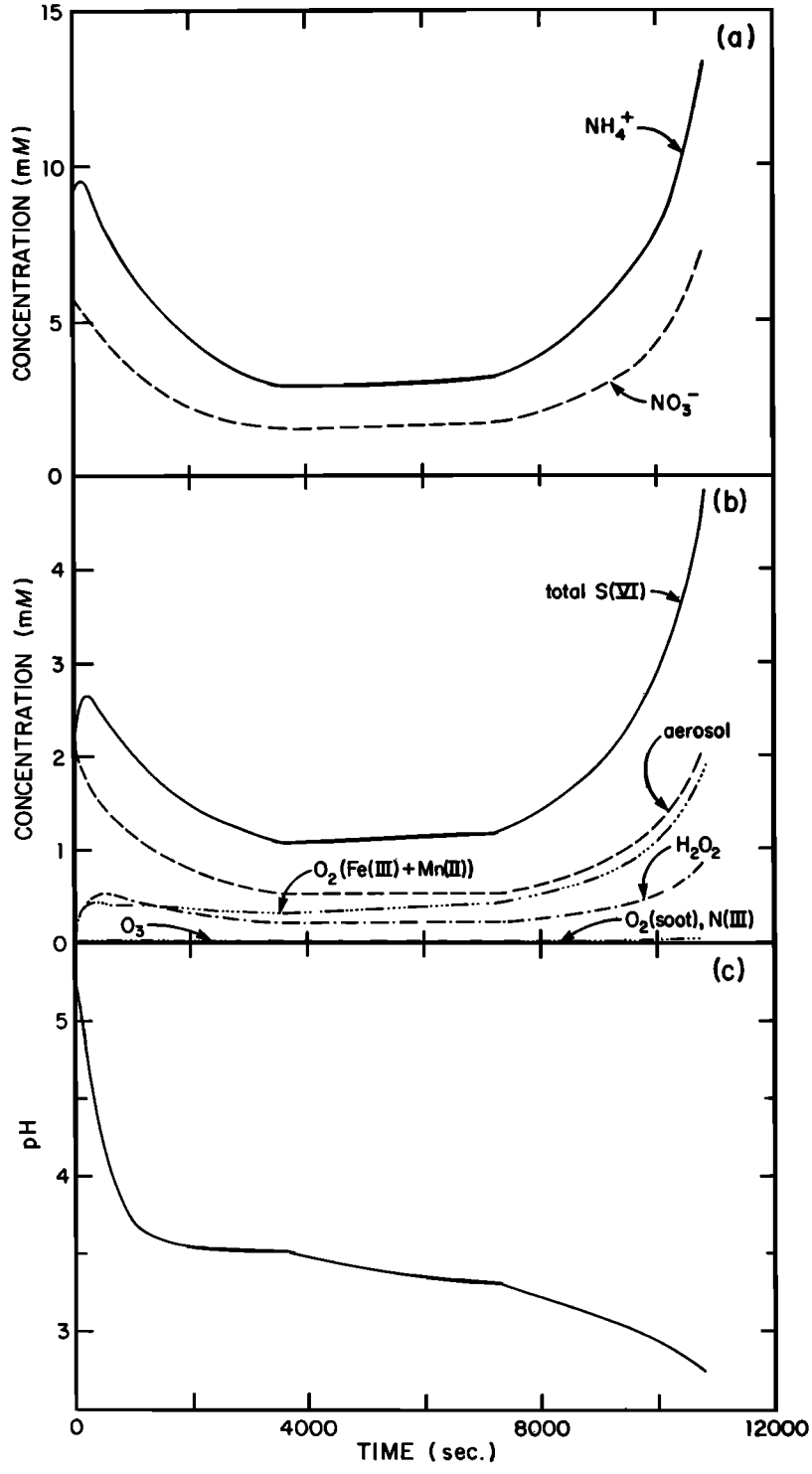

Fig. 10. Profiles versus time of the concentrations of the major ions in the fogwater under conditions of Table 3, with liquid water content as given in Figure 9 and temperature = 10°C. (*a*) Nitrate and ammonium ions. (*b*) Total sulfate and individual contributions of the different sulfate production mechanisms. (*c*) *p*H.

the first few minutes of the fog. Hydroxymethanesulfonate is the major S(IV) species, and its formation may explain the high S(IV) levels found in fogwater [*Munger et al.*, 1983]. It should be noted that in addition to formaldehyde, sulfite is known to readily form sulfonates with other aldehydes, some of which have been found in fog at concentrations comparable to formaldehyde [*Grosjean and Wright*, 1983]. These reactions would further explain the high S(IV) concentrations observed.

Conclusion

The chemistry of fogs forming in an urban environment has been investigated using a hybrid kinetic and equilibrium model. The most important conclusions are as follows.

1. Aqueous phase oxidation of S(IV) is an important source of sulfate in the droplet. The principal oxidants are H_2O_2 and O_2 (catalyzed by Fe(III) and Mn(II)), although ozone can also be an important oxidant above *p*H 5. Oxida-

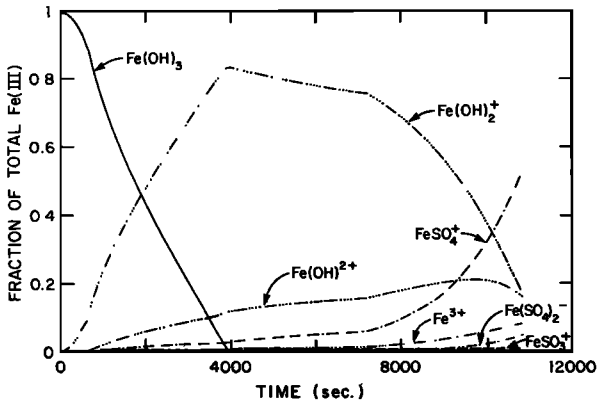

Fig. 11. Speciation of Fe(III) in the fogwater as a function of time under conditions of Table 3, with liquid water content as given in Figure 9 and temperature = 10°C.

tion by H_2O_2 is very fast but limited by its availability in the atmosphere. Most of the sulfate production occurs within the first hour following fog formation.

2. When fog condenses on alkaline to slightly acid nuclei, important acidification occurs as a result of S(IV) oxidation. In the first case simulated, the *p*H dropped two units from its initial value of 5.5 during the first half hour of the fog; it then stabilized around *p*H 3. When the fog formed on highly acidic condensation nuclei, however, the *p*H drop due to S(IV) oxidation was very small because of the high acidity initially present in the droplet.

3. Oxidation of N(III) in the droplet does not lead to significant production of nitrate. Production of nitrate proceeds through gas phase formation of HNO_3 followed by dissolution and dissociation in the droplet. Nitric acid is scavenged efficiently by the droplets as it is formed in the gas phase.

4. NH_4^+ concentration is dependent both on the liquid water content of the fog and the solubility of NH_3. Below *p*H 5 the droplets are essentially a total sink for NH_3, but above *p*H 5 the gas is partitioned between the two phases in a highly *p*H-dependent manner.

5. Over 90% of the S(IV) present in the droplet is complexed as HMSA, and this may explain the high S(IV) concentrations observed by *Munger et al.* [1983]. Formation of HMSA releases free acidity, but its effect on the droplet *p*H is negligible.

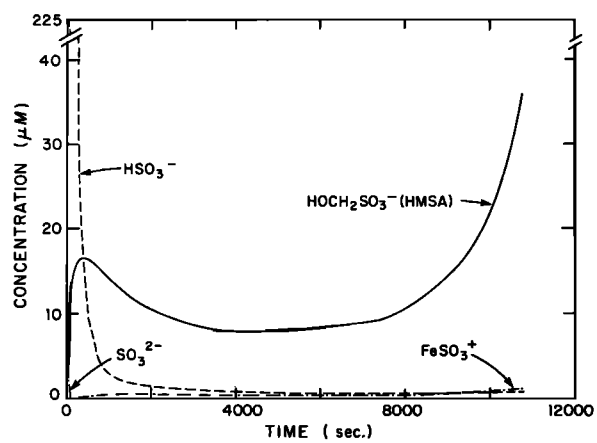

Fig. 12. Concentrations of S(IV) species in the fogwater as a function of time under conditions of Table 3, with liquid water content as given in Figure 9 and temperature = 10°C.

6. Fog does not affect the SO_2 gas phase concentrations greatly; as a result the supply of reactive S(IV) species for S(VI) and HMSA formation is determined primarily by the droplet *p*H. S(VI) formation proceeds faster than HMSA formation at all times and limits HMSA formation by causing the *p*H to drop and thus reducing the S(IV) supply.

7. At lower temperatures (1°C versus 10°C), metal-catalyzed oxidation by O_2 is slower and the importance of ozone as an S(IV) oxidant increases. Overall, sulfate and acidity are not produced as fast in the early stages of the fog but catch up later and become comparable in the later stage of the fog. Much more HMSA is produced at the lower temperature.

The model has thus revealed some important features of the chemistry and production of acidity in urban fogs. Gas phase and aerosol chemistry, droplet microphysics, and wind fields will have to be incorporated in future versions to give the simulations a predictive capability. These theoretical advances will have to be accompanied by concomitant sets of field measurements.

REFERENCES

Adamowicz, R. F., A model for the reversible washout of sulfur dioxide, ammonia and carbon dioxide from a polluted atmosphere and the production of sulfates in raindrops, *Atmos. Environ.*, *13*, 105–121, 1979.

Appel, B. R., E. L. Kothny, E. M. Hoffer, and J. J. Wesolowski, Sulfate and nitrate data from the California Aerosol Characterization Experiment (ACHEX), *Adv. Environ. Sci. Technol.*, *9*, 315–335, 1980.

Baboolal, L. B., H. R. Pruppacher, and J. H. Topalian, A sensitivity study of a theoretical model of SO_2 scavenging by water drops in air, *J. Atmos. Sci.*, *38*, 856–870, 1981.

Brimblecombe, P., and D. J. Spedding, The catalytic oxidation of micromolar aqueous sulphur dioxide, *Atmos. Environ.*, *8*, 937–945, 1974.

Brodzinsky, R., S. G. Chang, S. S. Markowitz, and T. Novakov, Kinetics and mechanism for the catalytic oxidation of sulfur dioxide on carbon in aqueous suspensions, *J. Phys. Chem.*, *84*, 3354–3358, 1980.

Carmichael, G. R., T. Kitada, and L. K. Peters, The effects of in-cloud and below-cloud scavenging on the transport and gas phase reactions of SO_x, NO_y, HC_x, H_xO_y, and O_3 compounds, in *4th International Conference on Precipitation Scavenging, Dry Deposition, and Resuspension*, Santa Monica, December 1982, Elsevier, New York, in press, 1983.

Cass, G. R., Dimensions of the Los Angeles SO_2/sulfate problem, *Environ. Qual. Lab. Memo. 15*, Calif. Inst. of Technol., Pasadena, 1975.

Chameides, W. L., and D. D. Davis, The free radical chemistry of cloud droplets and its impact upon the composition of rain, *J. Geophys. Res.*, *87*, 4863–4877, 1982.

Dämschen, D. E., and L. R. Martin, Aqueous aerosol oxidation of nitrous acid by O_2, O_3, and H_2O_2, *Atmos. Environ.*, in press, 1983.

Dasgupta, P. K., K. De Cesare, and J. C. Ullrey, Determination of atmospheric sulfur dioxide without tetrachloromerurate(II) and the mechanism of the Schiff reaction, *Anal. Chem.*, *52*, 1912–1922, 1980.

Durham, J. L., J. M. Overton, and V. P. Aneja, Influence of gaseous nitric acid on sulfate production and acidity in rain, *Atmos. Environ.*, *15*, 1059–1068, 1981.

Easter, R. C., and P. V. Hobbs, The formation of sulfate and the enhancement of cloud condensation nuclei in clouds, *J. Atmos. Sci.*, *31*, 1586–1594, 1974.

Erickson, R. E., L. M. Yates, R. L. Clark, and D. McEwen, The reaction of sulfur dioxide with ozone in water and its possible atmospheric significance, *Atmos. Environ.*, *11*, 813–817, 1977.

Gartrell, G., Jr., S. L. Heisler, and S. K. Friedlander, Relating particulate properties to sources: The results of the California Aerosol Characterization Experiment, *Adv. Environ. Sci. Technol.*, *9*, 665–713, 1980.

Graedel, T. E., L. A. Farrow, and T. A. Weber, Kinetic studies of the photochemistry of the urban atmosphere, *Atmos. Environ.*, *10*, 1095–1116, 1976.

Graedel, T. E., P. S. Gill, and C. J. Wechsler, Effects of organic surface films on the scavenging of atmospheric gases by raindrops and aerosol particles, in *4th International Conference on Precipitation Scavenging, Dry Deposition, and Resuspension, Santa Monica, December 1982*, Elsevier, New York, in press, 1983.

Graham, R. A., and H. S. Johnston, The photochemistry of NO_3 and the kinetics of the N_2O_5–O_3 system, *J. Phys. Chem., 82*, 254–268, 1978.

Grosjean, D., Formaldehyde and other carbonyls in Los Angeles ambient air, *Environ. Sci. Technol., 16*, 254–262, 1982.

Grosjean, D., and B. Wright, Carbonyls in urban fog, ice fog, cloudwater and rain water, *Atmos. Environ.*, in press, 1983.

Hanst, P. L., N. W. Wong, and J. Bragin, A long-path infra-red study of Los Angeles smog, *Atmos. Environ., 16*, 969–981, 1982.

Hegg, D. A., and P. V. Hobbs, Cloudwater chemistry and the production of sulfates and clouds, *Atmos. Environ., 15*, 1597–1604, 1981.

Hoffmann, M. R., Thermodynamic, kinetic and extrathermodynamic considerations in the development of equilibrium models for aquatic systems, *Environ. Sci. Technol., 15*, 345–353, 1981.

Hoffmann, M. R., and D. J. Jacob, Kinetics and mechanisms of the catalytic oxidation of dissolved sulfur dioxide in aqueous solution: An application to nighttime fogwater chemistry, in *Acid Precipitation*, edited by J. G. Calvert, Ann Arbor Science, Ann Arbor, Mich., in press, 1983.

Jiusto, J. E., and G. G. Lala, Radiation fog field programs—Recent studies, *ASRC-SUNY Publ. 869*, State Univ. of N. Y., Albany, 1983.

Landolt-Börnstein, *Zahlenwerte und Funktionen. Gleichgewicht der Absorption von Gasen in Flüssigkeiten von niedrigem Dampfdruck*, 6th ed., vol. 4, part 4, sect. C, Springer Verlag, Heidelberg, Federal Republic of Germany, 1976.

Ledbury, W., and E. W. Blair, The partial formaldehyde vapour pressure of aqueous solutions of formaldehyde, 2, *J. Chem. Soc., 127*, 2832–2839, 1925.

Liljestrand, H. M., and J. J. Morgan, Spatial variations of acid precipitation in Southern California, *Environ. Sci. Technol., 15*, 333–339, 1981.

Maahs, H. G., The importance of ozone in the oxidation of sulfur dioxide in nonurban tropospheric clouds, paper presented at the 2nd Symposium on the Composition of the Nonurban Troposphere, Am. Meteorol. Soc., Williamsburg, Va., 1982.

Martin, L. R., Kinetic studies of sulfite oxidation in aqueous solution, in *Acid Precipitation*, edited by J. G. Calvert, Ann Arbor Science, Ann Arbor, Mich., in press, 1983.

McRae, G. J., Mathematical modeling of photochemical air pollution, Ph.D. thesis, Calif. Inst. of Technol., Pasadena, 1981.

McRae, G. J., and A. G. Russell, Dry deposition of nitrogen containing species, in *Acid Deposition: Wet and Dry*, vol. 6, edited by B. B. Hicks, Ann Arbor Science, Ann Arbor, in press, 1983.

Middleton, P., C. S. Kiang, and V. A. Mohnen, Theoretical estimates of the relative importance of various urban sulfate aerosol production mechanisms, *Atmos. Environ., 14*, 463–472, 1980.

Morel, F., and J. J. Morgan, A numerical method for computing equilibria in aqueous chemical systems, *Environ. Sci. Technol., 6*, 58–67, 1972.

Munger, J. W., D. J. Jacob, J. M. Waldman, and M. R. Hoffmann, Fogwater chemistry in an urban atmosphere, *J. Geophys. Res., 88*, 5109–5121, 1983.

Oblath, S. B., S. S. Markowitz, T. Novakov and S. C. Chang, Kinetics of the formation of hydrozylamine disulfonate by reaction of nitrite with sulfites, *J. Phys. Chem., 85*, 1017–1021, 1981.

Perry, J. M., *Chemical Engineer's Handbook*, 4th ed., McGraw-Hill, New York, 1963.

Richards, L. W., J. A. Anderson, D. L. Blumenthal, J. A. McDonald, G. L. Kok, and A. L. Lazrus, Hydrogen peroxide and sulfur (IV) in Los Angeles cloud water, *Atmos. Environ.*, 17, 911–914, 1983.

Roberts, J. D., R. Stewart, and M. C. Caserio, *Organic Chemistry*, W. A. Benjamin, Menlo Park, Calif., 1971.

Russell, A. G., G. J. McRae, and G. R. Cass, Mathematical modeling of the formation and transport of ammonium nitrate aerosol, *Atmos. Environ.*, in press, 1983.

Schwartz, S. E., Gas-aqueous reactions of sulfur and nitrogen oxides in liquid-water clouds, in *Acid Precipitation*, edited by J. G. Calvert, Ann Arbor Science, Ann Arbor, Mich., in press, 1983.

Schwartz, S. E., and J. E. Freiberg, Mass-transport limitation to the rate of reaction of gases in liquid droplets: Application to oxidation of SO_2 in aqueous solutions, *Atmos. Environ., 15*, 1129–1144, 1981.

Schwartz, S. E., and W. H. White, Solubility equilibria of the nitrogen oxides and oxyacids in dilute aqueous solution, *Adv. Environ. Sci. Eng., 4*, 1–45, 1981.

Sillén, G. L. and A. E. Martell, Stability constants of metal-ion complexes, *Spec. Publ. 17*, Chem. Soc., London, 1964.

Sørensen, P. E., and V. S. Andersen,, The formaldehyde-hydrogen sulphite system in alkaline aqueous solution: Kinetics, mechanisms, and equilibria, *Acta Chem. Scand., 24*, 1301–1306, 1970.

Stumm, W., and J. J. Morgan, *Aquatic Chemistry*, 2nd ed., Wiley-Interscience, New York, 1981.

Waldman, J. M., J. W. Munger, D. J. Jacob, R. C. Flagan, J. J. Morgan, and M. R. Hoffmann, Chemical composition of acid fog, *Science, 218*, 677–680, 1982.

Westall, J. C., J. L. Zachary, and F. M. Morel, MINEQL, a computer program for the calculation of chemical equilibrium composition of aqueous solutions, *Tech. Note 18*, Dep. of Civ. Eng., Mass. Inst. of Technol., Cambridge, Mass., 1976.

(Received October 4, 1982;
revised April 14, 1983;
accepted April 14, 1983.)